Application note

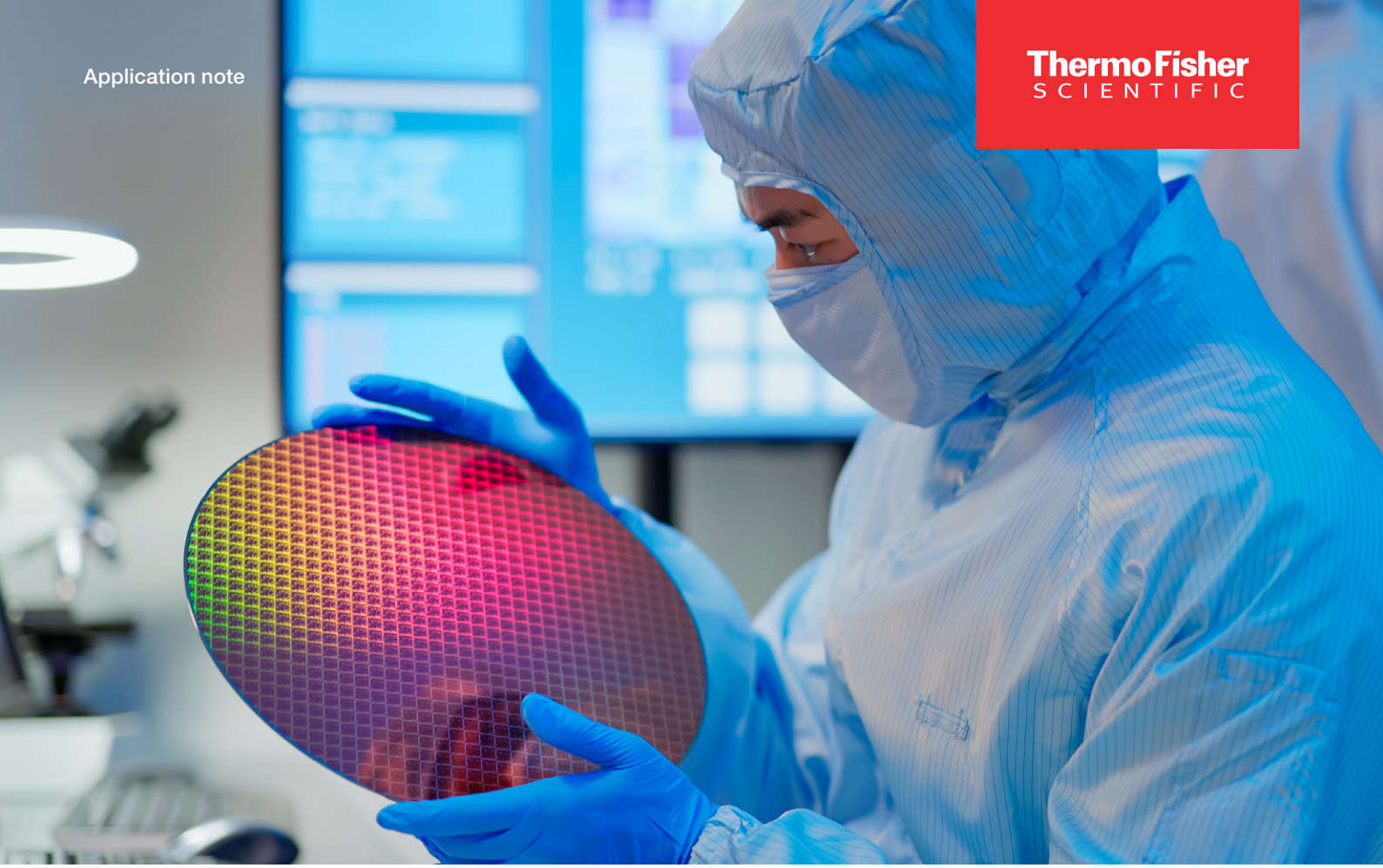

Using Raman spectroscopy to determine the strain in semiconductor samples

Authors

Maximilian Ries, Thermo Fisher Scientific GmbH, and Fabian Heisinger, Technische Universität Berlin

Raman spectroscopy is highly sensitive to subtle changes in a material's crystal lattice structure. When a semiconductor is strained, under pressure or tension, its molecular bonds shift slightly, altering the vibrational frequencies of the lattice vibrations. By measuring the resulting shifts in Raman peaks, the amount and type of strain present in the semiconductor material can be deduced. Such information is crucial in semiconductor technology, as even small amounts of strain can significantly impact the material's properties and affect device performance. Examples of possible effects caused by strain on semiconductor devices include improved carrier mobility[1], changes to compatibility with existing technology[2], alterations in the tuning of material properties[3], and the ability to use strain engineering to allow for miniaturization[4] and site control.

This application note reports the strain analysis by Raman imaging of site-controlled quantum dots (SC-QDs) for integration into nanophotonic systems[5]. The scalability of such systems is critical for their incorporation into wide-ranging applications such as optoelectronics, quantum computing, and sensing. The integration of quantum dots into the systems can be optimized by fabrication techniques such as site-selective growth or buried stressor methods. These techniques offer precise positioning and number control of desired quasi-zero-dimensional gain centers like InGaAs quantum dots.

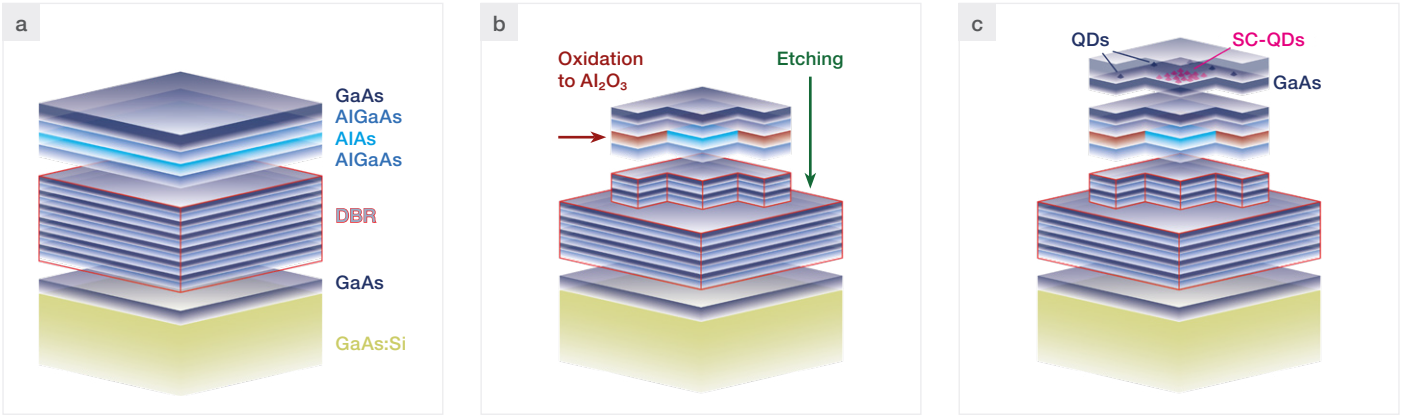

Figure 1. (a) The initial epitaxy step involves growing a template structure of a 300 nm GaAs buffer layer, 15 pairs of GaAs/$Al_{0.9}Ga_{0.1}As$ distributed Bragg reflector (DBR), a 30 nm AlAs stressor layer, and an 80 nm GaAs cap. (b) Following the UV lithography and etching steps, selective wet oxidation of AlAs to Al_2O_3 results in a precisely controlled unoxidized AlAs aperture in the center. (c) The second growth step adds a 50 nm GaAs layer followed by the InGaAs QD-layer. The strain emanating from the aperture induces the accumulation of indium atoms and enables site-controlled nucleation of QDs (SC-QDs) above the aperture.

The SC-QDs sample analyzed herein was grown via Metal-Organic Chemical Vapor Deposition on a GaAs:Si wafer and consists of three parts: an AlGaAs/GaAs distributed Bragg reflector (DBR) template to enhance the extraction efficiency; the stressor layer consisting of 30 nm of aluminum arsenide (AlAs); and the final layer of a 1.8 monolayer-thick QD-layer of In(0.63)Ga(0.37)As in a GaAs matrix (Figure 1). The fabrication involves five steps: the growth of the template and the stressor layer; lithographical patterning; dry etching; oxidation of the AlAs layer; and the growth of the QD-layer. In the second step, lithographically defined arrays of approx. 20 µm squares (mesas) with 63 nm step size are written on the template via plasma-enhanced reactive ion etching. In the third step, the AlAs layer is oxidized to Al_2O_3 from the sides to form the AlAs aperture in the center of the mesas. This oxidation process is highly selective to AlAs and does not affect the rest of the structure. Due to the different lattice constants of AlAs and Al_2O_3, lateral stress results in a strain profile on the surface. In the final step, QDs grow preferably on tensile strained positions. Moreover, the strain emanating from the stressor layer induces curvature in any layer grown on top of the QDs. In the case of a top DBR, this curvature results in three-dimensional confinement, giving rise to cavity modes. These modes show lasing behaviors, eliminating the need for an additional processing step to pattern microlasers.

Thermo Scientific DXR3xi Raman Imaging Microscope.

A Thermo Scientific™ DXR3xi Raman Imaging Microscope was employed to monitor the distribution of strain using a 532 nm green diode-pumped solid-state laser with a maximum excitation power of 10 mW. The laser was focused onto the sample through a 0.9 NA Olympus MPlan 100x objective. To enhance the spatial resolution, a 25 µm confocal pinhole was used. The spectrometer was equipped with a high-resolution grating with an absolute spectral resolution of 2 cm^{-1} and an electron-multiplying charge-coupled device (EMCCD) for spectrum recording. Data collection and analysis were performed using Thermo Scientific™ OMNICxi Software.

A scanning area of 6 µm x 6 µm centered around the aperture was recorded with a step size of 100 nm. The laser power was set at 2 mW to avoid damage by localized heating. A typical spectrum is shown in Figure 2. For each Raman spectrum, a Lorentzian function was employed to fit the GaAs longitudinal optical (LO) phonon (292 cm^{-1}) and the AlAs LO phonon (400 cm^{-1}). The impact of the strain from the AlAs aperture is manifested by the frequency shift of the GaAs LO phonon due to the strain-induced lattice distortion.

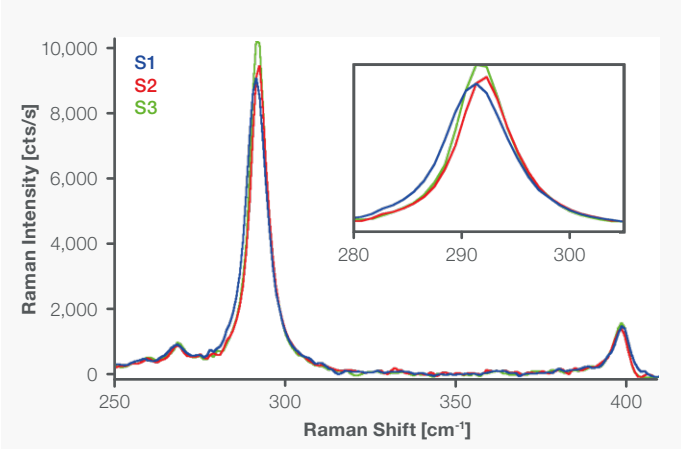

Figure 2. Raman spectra of the SC-QD sample with an AlAs aperture of 0.74 µm. The GaAs longitudinal optical phonon is at 292 cm^{-1} and the AlAs LO phonon is at 400 cm^{-1}. The inset shows a zoom-in to the GaAs phonon band.

Through Raman imaging, each position of the sample is assigned with its distinct GaAs LO phonon frequency value $\omega(LO)_{xy}$. The resulting Raman maps with $\omega(LO)_{xy}$ is shown in Figure 3 for three different sized AlAs apertures. From left to right in Figure 3a, the frequency first increases, then drops significantly, and reaches the minimum frequency value in the center of the aperture. For larger apertures, the frequency reaches the nominally unstrained value around the center of the aperture. Furthermore, it becomes obvious that the variation of the frequency is well below the absolute spectral resolution, which is nominally 2 cm^{-1}. The relative shift of this band can be determined with a precision approximately 40x better than the absolute spectral resolution.[6] The frequency shift is the difference between $\omega(LO)_{xy}$ and the unstrained GaAs frequency $\omega(LO)_{GaAs}$. It is denoted as $\Delta\omega(LO)_{xy}=\omega(LO)_{GaAs}-\omega(LO)_{xy}$. This measurable quantity is related to a strain value as given in Equation (1)[7], where ε_p is the parallel strain in %:

$$\Delta\omega(LO)_{xy} = -485\ \varepsilon_p$$

Equation 1.

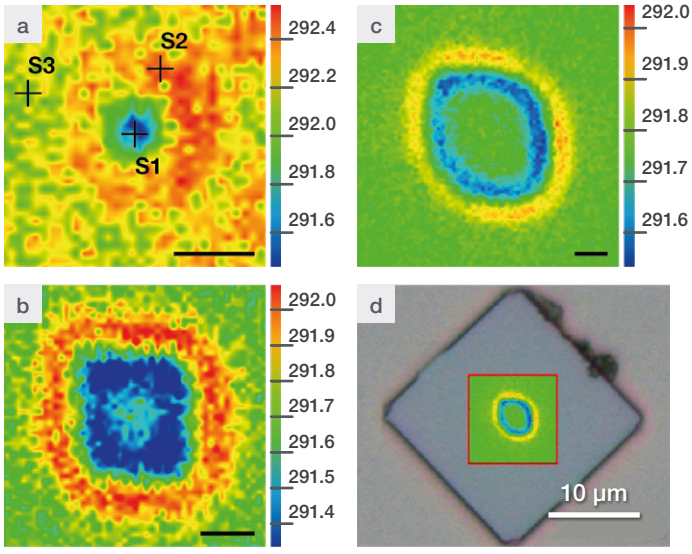

Figure 3. Spatial distribution of the GaAs LO-phonon frequency in cm^{-1} around three different AlAs aperture in the center of the mesa-structures. The width of the aperture region was determined by AFM to (a) 0.74 µm; (b) 2.36 µm; and (c) 4.08 µm. The scale bars in the figures correspond to 1 µm, respectively. In (d) a microscope image of the 2.36 µm aperture with the overlaid Raman image is shown.

Figure 3 represents an estimation of the strain distribution across the overgrown AlAs aperture based on the frequency value of the GaAs LO-phonon. Using Equation (1), the frequency shifts across the apertures were converted to the strain values, and the results were plotted in Figure 4. The Raman strain profiles and the AFM height profiles show great agreement. A reduction of the AlAs layer width results in a more localized site selection with higher strain, while larger apertures yield a larger, square-shaped distribution of emitters with lower density and less pronounced redshift of the SC-QD luminescence. Moreover, the stress is highest at the edges of the aperture, where the lattice is "bent" across the edges. Conversely, in the center of the structure the stress relaxes, which can be seen in the profile of the largest structure where the stress goes back to zero. The difference between the shape of the AFM profile and the Raman profile is due to the spatial resolution of the respective technique and the relaxation of the stress across the aperture. While the spatial resolution in AFM largely depends on the sharpness of the tip and is typically of the order of 10 nm and below. For Raman microscopy, the spatial resolution depends primarily on the size of the laser spot and is approximately 500 nm.

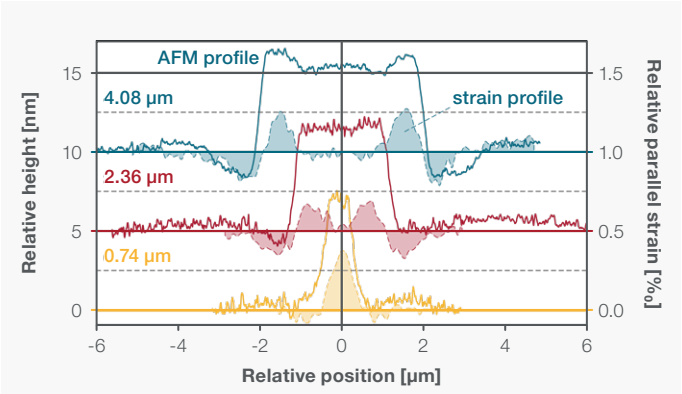

Figure 4. Different aperture sizes of 0.74 – 4.08 µm assessed with AFM height profiles (left axis, solid lines) and Raman profiles of the strain (right axis, filled curves with broken lines). The profiles are offset with respect to each other for better perception.

In this application note, it is demonstrated that Raman microscopy is a powerful technique for material characterization. The spatial distribution of the strains across AlAs apertures, extracted from the strain-induced GaAs LO-phonon frequency shift, provides valuable information for the assessment of growth parameters in the fabrication of semiconductor devices and thus provides information about how strain can affect device performance.

References

1. N. Mohta and S. E. Thompson, "Mobility enhancement," IEEE Circuits and Devices Magazine, vol. 21, no. 5, pp. 18–23, Sep. 2005, doi: 10.1109/mcd.2005.1517386.
2. Man Ho Kwan et al., "CMOS-compatible GaN-on-Si field-effect transistors for high voltage power applications," 2014 IEEE International Electron Devices Meeting, Dec. 2014, doi: 10.1109/iedm.2014.7047073
3. D. V. Lang, R. People, J. C. Bean, and A. M. Sergent, "Measurement of the band gap of GexSi1–x/Si strained-layer heterostructures," Applied Physics Letters, vol. 47, no. 12, pp. 1333–1335, Dec. 1985, doi: 10.1063/1.96271.
4. J. Martín-Sánchez et al., "Strain-tuning of the optical properties of semiconductor nanomaterials by integration onto piezoelectric actuators," Semiconductor Science and Technology, vol. 33, no. 1, p. 013001, Dec. 2017, doi: 10.1088/1361-6641/aa9b53.
5. I. Limame, F. Heisinger et al., "Epitaxial growth and characterization of multi-layer site-controlled InGaAs quantum dots based on the buried stressor method," Applied Physics Letters, vol. 124, no. 6, Feb. 2024, doi: 10.1063/5.0187074.
6. J. Hodkiewicz and F. Deck, "Evaluating Spectral Resolution on a Raman Spectrometer," Thermo Fisher Scientific, Technical Note: 52043
7. G. Attolini et al., "Raman scattering study of residual strain in GaAs/InP heterostructures," Journal of Applied Physics, vol. 75, no. 8, pp. 4156–4160, Apr. 1994, doi: 10.1063/1.355997.

Acknowledgment:

We gratefully acknowledge Imad Limame and the research group of Stephan Reitzenstein at the Technical University Berlin for conducting the study together and allowing for the usage of materials used in their publication.

Learn more at **thermofisher.com/DXR3xi**